Extended Release of Bevacizumab by Thermosensitive Biodegradable and Biocompatible Hydrogel

ARTICLE *in* BIOMACROMOLECULES · DECEMBER 2011

Impact Factor: 5.75 · DOI: 10.1021/bm2009558 · Source: PubMed

6 AUTHORS, INCLUDING:

Yih-Shiou Hwang
Chang Gung Memorial Hospital
62 PUBLICATIONS **371** CITATIONS
SEE PROFILE

Chia-Rui Shen
Chang Gung University
65 PUBLICATIONS **848** CITATIONS
SEE PROFILE

Article

pubs.acs.org/Biomac

Extended Release of Bevacizumab by Thermosensitive Biodegradable and Biocompatible Hydrogel

Chau-Hui Wang,[†,▽] Yih-Shiou Hwang,[*,‡,§,▽] Ping-Ray Chiang,[⊥] Chia-Rui Shen,[∥] Wei-Hsin Hong,[‡,∥] and Ging-Ho Hsiue[*,⊥,#]

[†]Polymer Technology Division, Material and Chemical Research Laboratories, Industrial Technology Research Institute, Hsinchu, 300 Taiwan, Republic of China

[‡]Department of Ophthalmology, Chang Gung Memorial Hospital, Linkou, 333 Taiwan, Republic of China

[§]Graduate Institute of Clinical Medical Sciences, College of Medicine and [∥]Department of Medical Biotechnology and Laboratory Science, Chang Gung University, Taoyuan, 333 Taiwan, Republic of China

[⊥]Department of Chemical Engineering, National Tsing Hua University, Hsinchu, 300 Taiwan, Republic of China

[#]Department of Chemical Engineering/R&D Center for Membrane Technology, Chung Yuan University, Chung Li, 320 Taiwan, Republic of China

ABSTRACT: The antibody bevacizumab (Avastin) has been used clinically to treat intraocular neovascular diseases based on its antivascular endothelial growth factor (VEGF) character. The anti-VEGF strategy for retinal neovascular diseases is limited by the short half-life of bevacizumab and thus requires frequent injections. This Article reports the sustained release of bevacizumab from a biocompatible material that is composed of a triblock copolymer of poly(2-ethyl-2-oxazoline)-*b*-poly(ε-caprolactone)-*b*-poly(2-ethyl-2-oxazoline) (PEOz-PCL-PEOz). The amphiphilic PEOz-PCL-PEOz triblock copolymer was synthesized in three steps. First, the PEOz was polymerized by methyl *p*-toluenesulfonate and 2-ethyl-2-oxazoline (EOz), and the living end was terminated by potassium hydroxide methanolic solution. Subsequently, the hydroxyl-PEOz was used as a macroinitiator for the ring-opening polymerization of ε-caprolactone using a Tin(II) octoate catalyst to synthesize the telechelic hydroxylated PEOz-PCL. Finally, the PEOz-PCL-PEOz triblock copolymer was obtained using the 1,6-hexamethylene diisocyanateas a coupling reagent. The PEOz-PCL-PEOz was chemically and molecularly characterized by GPC, ^{1}H NMR, and FTIR, and its aqueous solution (ECE hydrogel) showed a reversible sol (room temperature)−gel (physiological temperature) phase transition, which serves as an easy antibody-packing system with extended release. The biodegradability of ECE hydrogel was assessed by the porosity formation at different periods by scanning electron microscopy. The ECE hydrogel had no in vitro cytotoxicity on the human retinal pigment epithelial cell line by flow cytometry. The histomorphology and electrophysiology of the rabbit neuroretina were preserved after 2 months of intravitreal injection. In conclusion, the ECE hydrogel has a temperature-sensitive sol−gel phase transition and is effective in vitro. Its intraocular biocompatibility demonstrated its great potential to be widely used in biomedical applications for extended drug release.

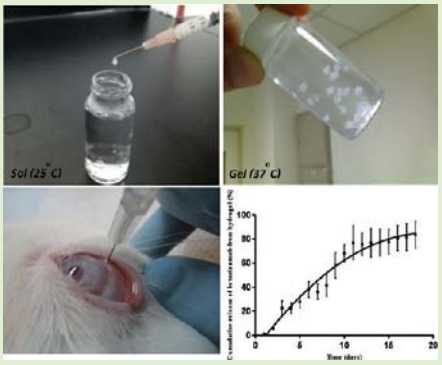

INTRODUCTION

Many of the major blinding diseases, such as proliferative diabetic retinopathy in diabetic patients, wet age-related macular degeneration (AMD) in older patients, and retinopathy of prematurity in premature newborns, have a common pathway of neovascularization. Vascular endothelial growth factor (VEGF) is the major cytokine for neovascular growth.[1] On the basis of the MARINA and ANCHOR studies, the anti-VEGF antibody ranibizumab has revolutionized the treatment strategy for neovascular AMD[2,3] and subsequently for other neovascular ocular diseases[4] when administered by intraocular injection.

Bevacizumab, a chimeric anti-VEGF antibody, is used to treat colon cancer by inhibiting tumor neovascularization, resulting in a higher survival rate.[5−7] Although bevacizumab intraocular injection is still off-label, it is also effective for intraocular neovascular disorders as ranibizumab, the open-label anti-VEGF drug.[4,8] The CATT research group reported that ranibizumab and bevacizumab have equivalent effects on visual acuity for neovascular AMD.[9] However, the low cost of bevacizumab makes it more widely used than ranibizumab all over the world.[10]

Although intravitreal injection of ranibizumab or bevacizumab is effective in neovascular inhibition and in improving vision, the short half-lives of these antibodies require frequent injections to maintain their therapeutic effect.[11] The PIER[12]

Received: July 10, 2011
Revised: December 3, 2011
Published: December 6, 2011

and SUSTAIN[13] studies demonstrated that when the frequency of injection decreased, the visual gain from injections would be lost. Nevertheless, frequent injections are inconvenient and carry a psychological burden and risk of infectious endophthalmitis, which is devastating to vision.[14] Because new antibody drugs are more and more commonly being used in many clinical applications, including immunology, tumor biology, and ophthalmology, attention has recently shifted from the development of new drugs to the development of strategies for extending the therapeutic effect of current drugs.[15,16] An extended half life by slowing the release of antibody drugs can improve the treatment effectiveness and also reduce costs.

Many approaches have been developed for sustained drug delivery using polymeric materials, such as microspheres,[17] nanoparticles,[18] micelles,[19] liposomes,[16] and hydrogels.[15] These delivery systems exhibit advantages of extended drug efficiency over the free drugs alone. We developed a thermosensitive poly(*N*-isopropylacrylamide-*g*-2-hydroxyethyl methacrylate) (PNIPAAm-*g*-PHEMA) hydrogel and thermosensitive PNIPAAm-*g*-PHEMA gel particles to formulate the antiglaucoma drug epinephrine in the form of a slow-releasing eyedrop. Animal experiments showed that this polymeric eye drop, which was formed by mixing (PNIPAAm-*g*-PHEMA) hydrogel, thermosensitive PNIPAAm-*g*-PHEMA gel particles, and epinephrine, can effectively extend the lowering effect in intraocular pressure (IOP) up to 26 h following administration, longer than that achieved with a traditional eye drop.[20] Kang Derwent et al. synthesized a biomaterial using PNIPAAm that was cross-linked with poly(ethylene glycol) diacrylate to form a thermosensitive hydrogel for encapsulating a protein drug as an injectable intravitreal drug delivery system.[15] However, the release of bovine serum albumin (BSA) from it showed an initial burst release of ~30%, which is unfavorable for the extended release profile. Turturro et al. also investigated the effects of thermosensitive hydrogel on neuroretinal tissue.[21] The result showed that *a*- and *b*-wave amplitudes of electroretinography (ERG) decreased 15% in 1 week after injection. Moreover, no significance could be obtained in the blood flow and optical coherent tomography (OCT) analysis at 1 week after injection. This study also suggested that the thermoresponsive hydrogel could be used as an intraocular drug-delivery platform.

Thermoresponsive and biodegradable hydrogels (TBHs) have been developed in recent years for sustained drug delivery and cell therapy to treat ocular diseases.[22−27] Most TBHs are composed of hydrophilic−hydrophobic block copolymers. Accordingly, their sol−gel transition can be controlled by adjusting their hydrophilicity/hydrophobicity balance. The sol−gel transition provides special advantages. For example, the drugs or cells can be manipulated in the lower temperature sol phase to prevent the denaturation of biomolecules. After injection into the body, the sol phase changes to the gel phase at body temperature (37 °C), which not only protects the drug from enzymatic degradation but also makes it possible to extend the release of drugs.[28−30] The degradability of these materials eliminates the need of surgery to remove residuals when all of the drug has been released.[31,32] To date, few studies have focused on TBHs for treatment of neovascular ocular diseases, which unfortunately are prevalent eye-blinding diseases throughout the world.

To extend the release of bevacizumab, we synthesized poly(2-ethyl-2-oxazoline)-*b*-poly(ε-caprolactone)-*b*-poly(2-ethyl-2-oxazoline) (PEOz-PCL-PEOz), and its aqueous solution (ECE hydrogel) was prepared to encapsulate bevacizumab. PEOz is a hydrophilic and biocompatible polymer. It has recently attracted attention for biomedical applications, like as a drug carrier in radionuclide therapy and tumor imaging.[33,34] Furthermore, Mero et al. reported that PEOz is suitable for low- or high-molecular-weight drug conjugation and delivery.[35] Therefore, PEOz may be used as an alternative to PEG. The FDA-approved biodegradable polyester PCL is used in humans as a contraceptive implant. Moreover, the degradation products of PCL exhibit weaker acidification than PLA and PGA. The acidic degradation products lower the pH value and induce nonbacterial inflammation.[36] Therefore, PEOz-PCL-PEOz contains both hydrophilic, biocompatible and biodegradable, hydrophobic polymer chain segments.

In this study, the ECE hydrogel was designed as a new TBH, and its ability to encapsulate and protect bevacizumab for extended release was investigated. This study addressed five major questions concerning the synthesis of PEOz-PCL-PEOz: the sol−gel phase transition behavior, the in vitro drug release of bevacizumab, the hydrolytic degradability, and the in vitro and in vivo cytotoxicity.

MATERIALS AND METHODS

Materials. 2-Ethyl-2-oxazoline (EOz, Aldrich), methyl *p*-toluenesulfonate (MeOTs, Aldrich), and ε-caprolactone (CL, Aldrich) were purified by distillation over CaH_2 (Acros) at a reduced pressure. Toluene (Tedia) was dried over CaH_2 before use. Stannous octoate ($Sn(Oct)_2$, Sigma), 1,6-hexamethylene diisocyanate (HMDI, Aldrich), ethyl acetate (EA, Tedia), diethyl ether (Tedia), dimethyl sulfoxide (DMSO, Tedia), tetrahydrofuran (THF, Tedia), balanced salt solution as the standard saline for intraocular use (BSS, Alcon), fetal bovine serum (FBS, Hazelton biological), ketamine hydrochloride and xylazine (Ketalar; Parke-Davis), bevacizumab (Avastin, Genentech/Roche), and other reagents were used as received. The age-19 human retinal pigment epithelial (ARPE-19) cell line was obtained from the Bioresource Collection and Research Center, Hsinchu, Taiwan.

Synthesis of Macroinitiator Hydroxyl-poly(2-ethyl-oxazoline) (PEOz-OH). Telechelic hydroxylated poly(2-ethyl-oxazline) (PEOz-OH) was synthesized by the cationic ring-opening polymerization of EOz (0.016 mol, 10 mL) using MeOTs (0.016 mol, 2.47 mL) as the initiator in toluene (20 mL) with stirring under reflux in a nitrogen atmosphere at 100 °C for 5 h. After polymerization, hydroxyl groups were introduced at the ends of PEOz using a 0.1 N KOH methanolic solution (197 mL) at 0 °C for 2 h.[37] The polymer methanolic-toluene solution was pressed through silica gel in a flush column of a length of 3.0 cm and an internal diameter of 4.0 cm to remove the salt and then precipitated in cooled and excess diethyl ether (500 mL). Vacuum-drying at 40 °C for 24 h yielded a light-yellow product. Gel permeation chromatography (GPC) was performed on Phenomenex Phenogel columns equipped with a refractive index detector. The mobile phase was THF at a flow rate of 1.0 mL/min (40 °C). The columns were calibrated using poly(methyl methacrylate) standards (Polymer Laboratories). The number-average molecular weight (M_n) and the polydispersity index (PDI) were determined by GPC technique. The chemical structure of PEOz was confirmed by ^{1}H NMR spectroscopy (500 MHz, $CDCl_3$, δ): 1.1 $CH_3(N(COCH_2-C\underline{H}_2)CH_2CH_2)$, 2.1−2.4 $CH_3(N(COC\underline{H}_2CH_3)CH_2CH_2)$, 3.0−3.1$C\underline{H}3(N(COCH2CH3)CH_2CH_2)$, and 3.4 $CH_3(N(COCH_2CH_3)-C\underline{H}_2C\underline{H}_2)$. The 10 mg PEOz was dissolved in THF and then coated on CaF_2 plates for FT-IR examinations. The 1633−1650 cm^{-1} signal, which corresponds to the C═O amide stretching, corroborated the structure.

Synthesis of Amphiphilic Diblock Copolymer (PEOz-PCL). The diblock of the PEOz-PCL block copolymer was synthesized by the ring-opening polymerization of CL with PEOz-OH as a macroinitiator and $Sn(Oct)_2$ as a catalyst. The M_n of the PEOz/PCL block copolymer was adjusted by controlling the feed ratios of PEOz and CL

dx.doi.org/10.1021/bm2009558 | *Biomacromolecules* 2012, 13, 40−48

monomers (as shown in Table 1). For the synthesis of E4C20E4, PEOz (0.009 mol, 7.67 g) was dissolved in 40 mL of toluene, and the

Table 1. Molecular Characteristics of the PEOz-PCL-PEOz Triblock Copolymer

block copolymers	(EOz/CL)[a]	in feed ratio (mol %) ratio	composition (mol %)[b] PEOz (M_n)[c]	PEOz-PCL (M_n)[c]	M_n[c]	M_w/M_n[c]
E4C20E4	0.865	0.859	435	1319	3553	1.28
E5C22E5	0.769	0.642	484	1642	4365	1.25

[a]Molar feed ratio of ε-caprolactone to the repeating units of PEOz-OH. [b]Calculated from ^{1}H NMR. [c]Determined by GPC.

Scheme 1

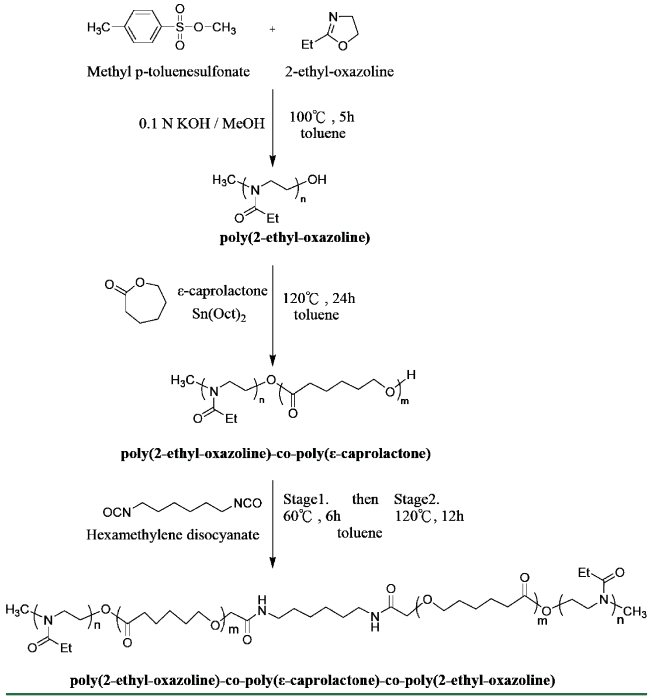

residual water was removed by azeotropic distillation to a final volume of 5 mL of polymer solution in toluene (PEOz-OH). Sequentially, 75 mL of anhydrous toluene was added to the flask under nitrogen. Then, 7.39 mL (0.067 mol) of CL was added to the PEOz-OH, and the temperature was increased gradually to 120 °C. Next, $Sn(Oct)_2$ (0.15 g) was added to the reaction, which proceeded for 24 h.[37,38] After the reaction proceeded to completion, the product was purified by first mixing with EA (200 mL), then was condensed in the evaporator to a 20 mL residual, and finally precipitated out in cooled diethyl ether. The precipitated product was vacuum-dried at 40 °C for 24 h, and the diblock copolymers (PEOz-PCL) were obtained. The chemical structure of PEOz-PCL was confirmed with ^{1}H NMR spectroscopy (500 MHz, $CDCl_3$, δ): 1.1 $CH_3(N(COCH_2C\underline{H}_3)CH_2CH_2)O(COCH_2CH_2CH_2CH_2CH_2O)H$, 1.3 $CH_3(N(COCH_2CH_3)CH_2CH_2)O(COCH_2CH_2C\underline{H}_2CH_2CH_2O)H$, 1.6–1.8 $CH_3(N(COCH_2CH_3)CH_2CH_2)O(COCH_2C\underline{H}_2CH_2C\underline{H}_2CH_2O)$ H, 2.1–2.4 $CH_3(N(COC\underline{H}_2CH_3)CH_2CH_2)O(COC\underline{H}_2CH_2CH_2CH_2CH_2O)H$, and 4.1$CH_3(N(COCH_2CH_3)CH_2CH_2)O(COCH_2CH_2CH_2CH_2C\underline{H}_2O)H$) and by FT-IR (1730 cm^{-1} C═O of ester, stretching; 1160 cm^{-1} C–O of ester, stretching; and 1640 cm^{-1} C═O of amide, stretching).

Coupling of Amphiphilic Diblock Copolymers (PEOz-PCL) to Form a Novel Thermosensitive Triblock Copolymer (PEOz-PCL-PEOz). The thermosensitive triblock copolymer (PEOz-PCL-

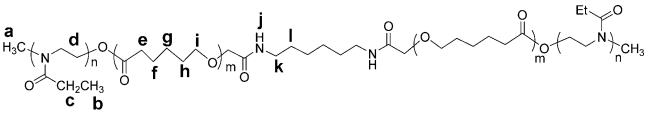

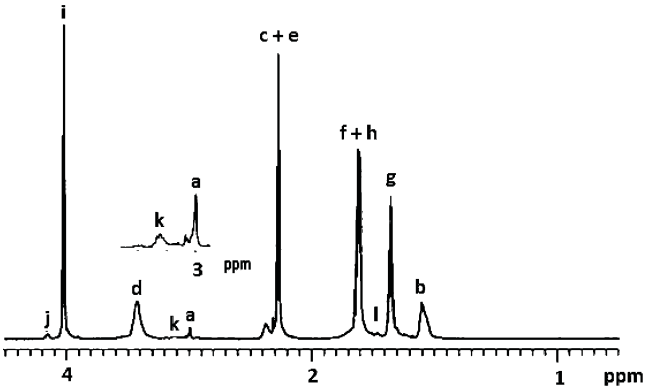

Figure 1. ^{1}H NMR spectrum of PEOz-PCL-PEOz triblock copolymer in $CDCl_3$.

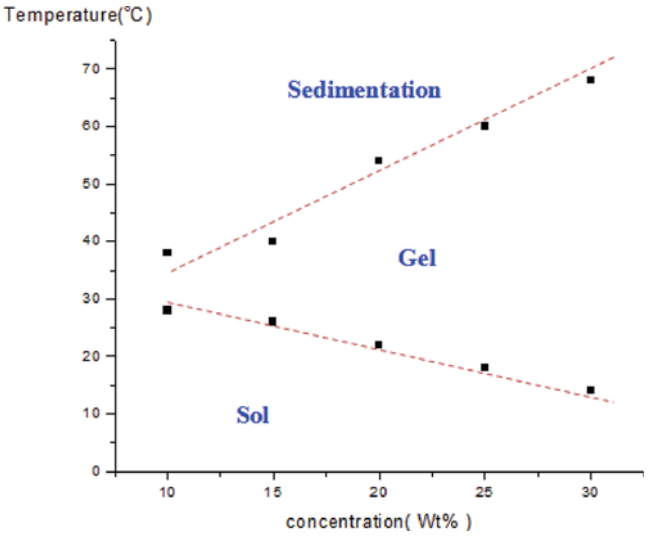

Figure 2. Temperature-sensitive sol–gel transition of PEOz-PCL-PEOz aqueous solutions at 10, 15, 20, 25, and 30 wt % concentrations.

PEOz) was formed by coupling two diblock copolymers with the hydroxyl groups of PEOz-PCL and the coupling agent HMDI. The PEOz-PCL (11.85 g) was reacted with HMDI (0.685 mL) in toluene (62.5 mL). The system was then heated in two steps: first, for 12 h at 60 °C and then for 6 h at 120 °C. Finally, 250 mL of EA was added, and the product was precipitated in cooled and excess diethyl ether (500 mL). The product was then dried at 40 °C in a vacuum oven overnight and dissolved in DMSO. This polymeric solution was purified by dialysis (MWCO 1000, Spectrum) and lyophilized. Characterization was performed using ^{1}H NMR spectroscopy (500 MHz, $CDCl_3$; δ 1.47 PEOz-PCL-CONH($CH_2C\underline{H}_2CH_2CH_2C\underline{H}_2CH_2$); 3.15 PEOz-PCL-CONH($C\underline{H}_2CH_2CH_2CH_2CH_2C\underline{H}_2$); and 4.18 PEOz-PCL-CON$\underline{H}$($CH_2CH_2CH_2CH_2CH_2CH_2$)) and by FT-IR (1730 cm^{-1} (C═O of ester, stretching) and 1640 cm^{-1} (C═O of amide, stretching).

Sol–Gel Transition Diagram. The PEOz-PCL-PEOz triblock copolymer was dissolved in BSS at room temperature in a 20 mL vial to form the ECE hydrogel at a range of concentrations (10 to 30% w/v) and then stored overnight at 4 °C in a refrigerator. Next, the ECE hydrogel was immersed in a water bath at 2 °C. The vial was maintained at each temperature for 2 min to equilibrate and was then inverted for 1 min. The sol (flow)–gel (no flow) transition was

dx.doi.org/10.1021/bm2009558 | Biomacromolecules 2012, 13, 40–48

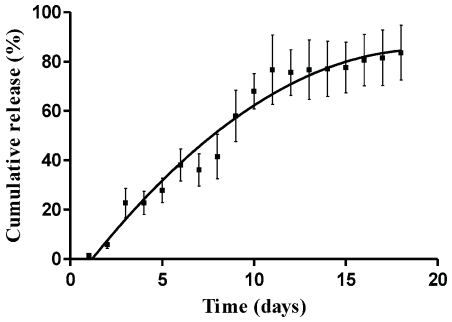

Figure 3. In vitro cumulative release curve of bevacizumab from 20 wt % ECE hydrogel.

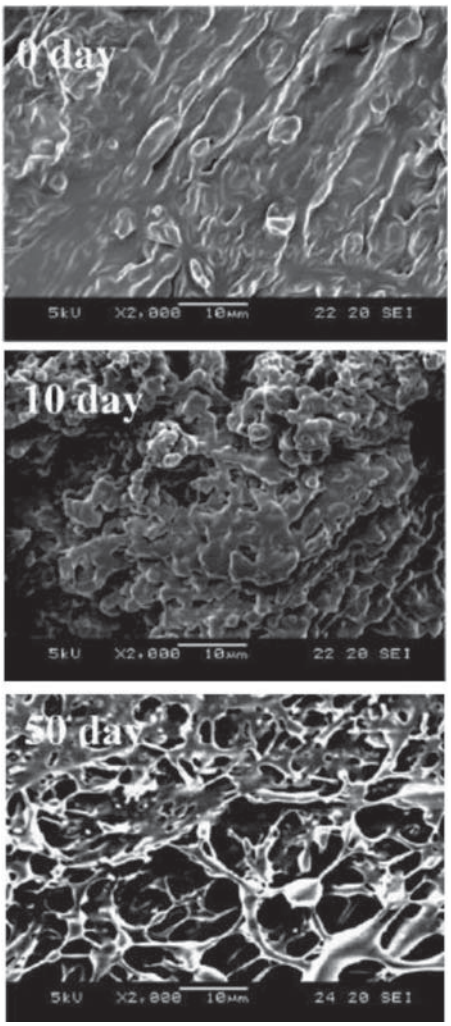

Figure 4. Scanning electron microscopy of 20 wt % ECE hydrogel after intervals of degradation times (0, 10, and 50 days) in BSS in a 37 °C water bath.

determined by the inversion method[31] in a water bath by increasing the temperature from 2 to 70 °C in 2 °C increments.

In Vitro Hydrolytic Degradability of ECE Hydrogel. The PEOz-PCL-PEOz triblock copolymer was dissolved in BSS at 20 wt % overnight at 4 °C; then, 0.05 mL of the ECE hydrogel was added to 4 mL of preheated BSS at 37 °C in a 20 mL vial. The samples were extracted at scheduled intervals and then freeze-dried. The hydrolytic degradability of the ECE hydrogel was determined by observing the morphology using scanning electron microscopy (SEM; Jeol JSM-5600).[30]

In Vitro Bevacizumab Encapsulation and Release. The PEOz-PCL-PEOz triblock copolymer was dissolved in BSS at 40% w/v overnight at 4 °C. Then, 0.05 mL of a bevacizumab solution (25 mg/mL) was mixed in a 1:1 (v/v) ratio with the ECE hydrogel and kept at low temperature (4 °C) to reach a final ECE concentration of 20% w/v. Next, 0.1 mL of the ECE hydrogel-bevacizumab solution was put in a 10 mL vial containing a flat-bottomed tube, with a fixed ECE hydrogel surface area, having a length of 1.3 cm and an internal diameter of 3 mm for 12 h in a bath at 37 °C to form a stable hydrogel. Then, 4 mL of BSS, which had been preheated to 37 °C, was injected into the vial. Next, 1.6 mL of the supernatant was periodically renewed with an equal volume of fresh BSS. The supernatant was collected as scheduled and frozen at −20 °C for the enzyme immunoassay. In brief, VEGF-coated polystyrene microplates were loaded with aqueous samples, washed, and incubated with horseradish peroxidase-conjugated rabbit antihuman IgG-Fc. After washing off the unbound conjugate and chromogenic substrate, tetramethylbenzidine (TMB) at a concentration of 0.4 g/L was added, and the absorbance was measured at 450 nm. Calibration curves were linear within the range from 0.425 to 15.25 mg/mL. The standard curves were verified with

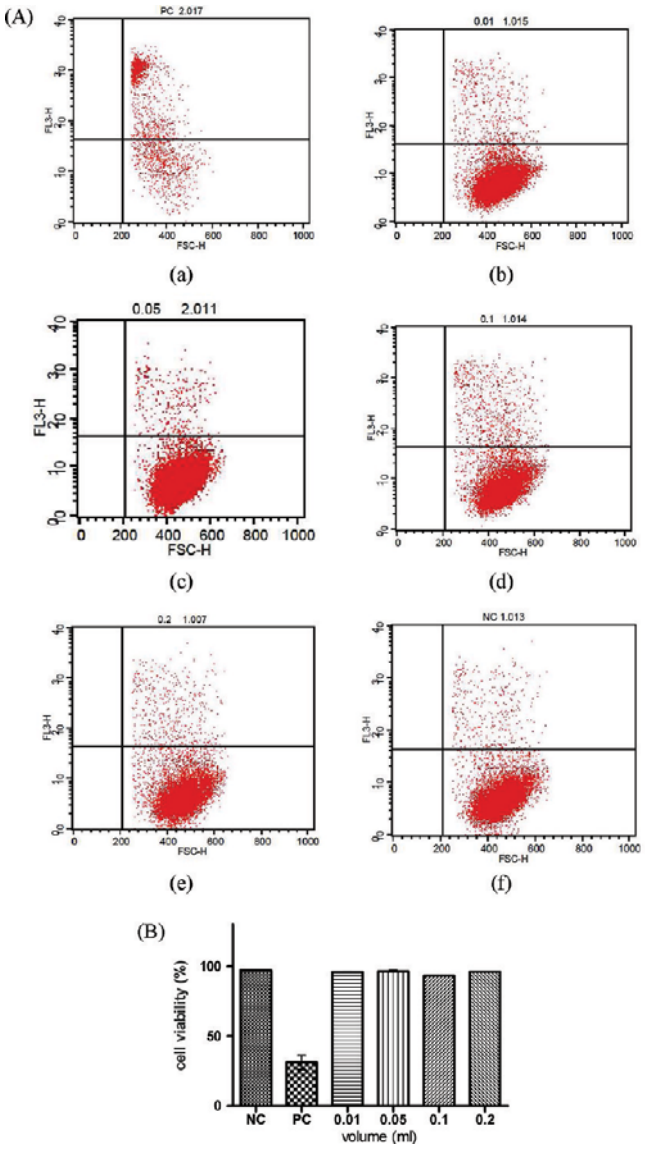

Figure 5. (A) (a) Cell viability of ARPE-19 cells by flow cytometric analysis, which was cultured in toxic CSPIO-containing medium as the positive control (P-Control), (b–e) cultured in different amounts (0.01, 0.05, 0.1, and 0.2 mL) of ECE-containing medium as the study group, and (f) cultured in medium only as the negative control (N-Control). (B) Cell viability percentage of ARPE-19 cocultured in the presence of ECE hydrogel of the different volumes noted above.

dx.doi.org/10.1021/bm2009558 | *Biomacromolecules* 2012, 13, 40–48

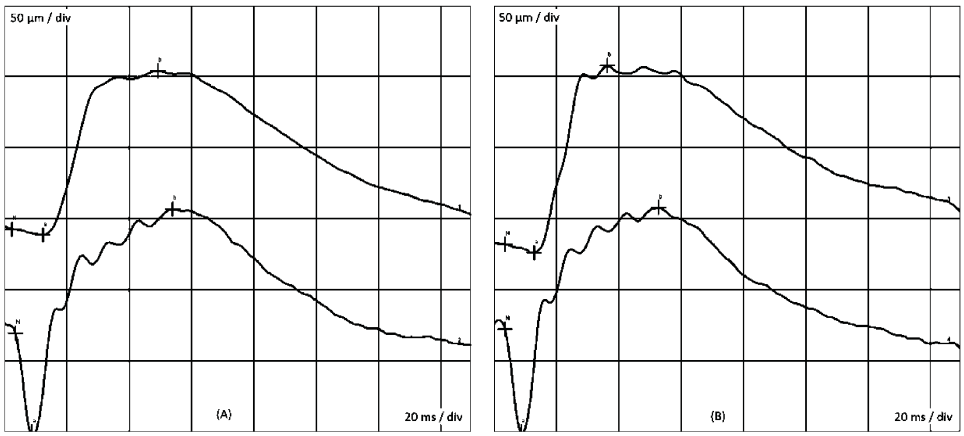

Figure 6. ERG waveforms before (left) and after (right) injection of ECE hydrogel into rabbit eyes.

various concentrations of bevacizumab solutions. All experiments were performed in triplicate.

In Vitro Cytotoxicity. To investigate the in vitro cytotoxicity of the ECE hydrogel, we filtered 0.01, 0.05, 0.1, and 0.2 mL of 20 wt % ECE hydrogel through a 0.22 μm filter for sterilization and then added to the ARPE-19 culture in the conventional six-well cell culture plate (Corning, USA) with 4 mL/well of the culture medium, a 1:1 mixture of DMEM (Dulbecco's modified Eagle's medium, Invitrogen, USA), and Ham's F12 (Invitrogen) with 2.5 mM L-glutamine (Invitrogen), supplemented with 10% FBS (Invitrogen), in a 5% CO_2 and 95% humidity incubator at 37 °C for 24 h. Because of the fluorescence of propidium iodide, which exclusively enters damaged cells, cell survival could also be measured by scoring the percentage of PI fluorescent-negative cells using a FACS Calibur System (Becton-Dickinson, San Jose, CA), as described elsewhere.[39] The experiments were performed in triplicate, and 10 000 events/cells were counted in each experiment. The known cytotoxic nanoparticles were added to some ARPE-19 cultures as the positive control.

Surgical Procedures and Intravitreal Injection of Rabbit Eyes. This investigation involved three male adult albino rabbits, each weighing between 2.5 and 3.0 kg. All of the experimental procedures followed the requirements for the Association for Research in Vision and Ophthalmology (ARVO) statement for the use of animals in ophthalmic and vision research as well as institutional guidelines. Three eyes of three rabbits (1 eye/each rabbit) received the in vivo intravitreal injection. The rabbits were anesthetized by intramuscular injection (0.5 mL/kg body weight) of a mixture of ketamine hydrochloride (10 mg/mL), acepromazine maleate solution (10%), and xylazine solution (2%) at a ratio of 1:0.2:0.3. Topical anesthesia (benoxinate HCl 0.4%) was administered to reduce the animals' discomfort. The pupils were fully dilated using 0.5% tropicamide and 2.5% phenylephrine hydrochloride. A levofloxacin ophthalmic solution was used to prevent infection, if necessary. A 500 μL single dose of 20 wt % ECE hydrogel-BSS (1:1 v/v) was sterilized by filtering through a 0.22 μm filter and then injected into the vitreous of the right eye using a 27-gauge microinjector under a dissecting microscope. The punch incision was made 1 mm posterior to the temporal limbus. The needle was inserted through the incision to a depth of 1.5 mm toward the optic nerve.

Electrophysiology of Retina. Full-field light-evoked ERG is a standard approach for evaluating the ocular toxicity of materials and drugs by checking the function of neurosensory retinas.[40] The ERG was conducted using a RETIport veterinary electrophysiological diagnostic system (Roland Consult, S&V Technologies AG, Germany) with an LED stimulation device attached to the electrode, which provided a bright-light maximum full intensity of 3.5 cds/m^2. An earring clip was placed on the ear lobe as a ground electrode after the hair in that region was shaved. The electrical impedance of all electrodes was <5 kΩ. Data were sampled at a rate of 1000 Hz, which was limited by band-pass filtering between 0.3 and 300 Hz. The ERG signals were amplified (5000×), and artifact signals associated with blinking were automatically removed. The ERG responses were initially recorded in a dark-adapted state after 30 min of dark adaptation and then in a light-adapted state with a background luminance of 25 cds/m^2. The ERG signal was analyzed offline using computer software (RETIport software version 5.0.0.1). ERG analysis of the flash responses was based on the wave amplitude. The *b*-wave amplitude was measured from the trough of the *a*-wave to the peak of the *b*-wave. The response of each studied eye was compared with that of itself before injection.

Ocular Histological Analysis. Histological analysis was performed to verify the in vivo cytotoxicity. The rabbits were euthanized 2 months after injection. Their eyes were enucleated, immersion-fixed in 4% formalin, and subsequently embedded in paraffin. We prepared 4 μm thick serial sections from paraffin blocks. Sections were deparaffinized and hydrated using sequential immersion in xylene and a graded alcohol solution. The sections were then mounted on glass slides and stained with hematoxylin and eosin. The slides were reviewed by two blinded independent observers in a random order and used for histological analysis.

Data Analysis. Descriptive statistics are presented as the mean ± standard deviation for continuous variables. Differences between two categorical and two far-from-normally distributed groups were evaluated using χ^2 and nonparametric analyses, respectively. Fisher's exact test for categorical groups was applied when counts within a category were <5. All statistical assessments were two-sided and evaluated at a significance level of 0.05.

■ RESULTS AND DISCUSSION

Synthesis and Characterization of PEOz-PCL-PEOz. Scheme 1 presents the method for synthesizing the amphiphilic PEOz-PCL-PEOz triblock copolymer. First, the PEOz was synthesized by cationic ring-opening polymerization of EOz with MeOTs as the initiator. MeOTs is an electrophilic initiator that preferentially attacks the nitrogen atom of the EOz ring to form oxazolinium. Adding more EOz continuously to oxazolinium results in chain propagation until all of the EOz is consumed. The polymer chain propagation can be terminated by a nucleophile substance.[41] In this study, the telechelic hydroxylated PEOz was obtained by end-capping the living cationic polymer chain with the addition of potassium hydroxide solution to functionalize the polymer further. Subsequently, PEOz-OH was used as a macroinitiator for the ring-opening polymerization of CL with an $Sn(Oct)_2$ catalyst to yield the telechelic hydroxylated PEOz-PCL. The PEOz-PCL-PEOz triblock copolymer was obtained by coupling the PEOz-PCL block copolymer using HMDI as a coupling reagent. Table 1 demonstrates two products that were obtained. The E4C20E4

dx.doi.org/10.1021/bm2009558 | *Biomacromolecules* 2012, 13, 40−48

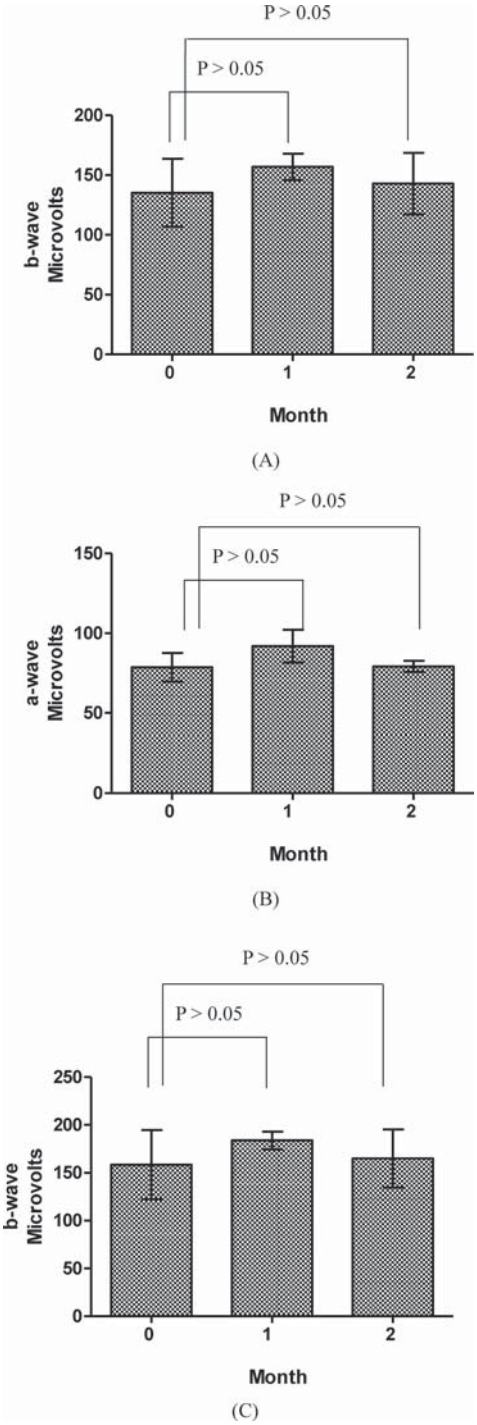

Figure 7. Scotopic ERG of rabbit eyes measured with bright (0.8 cd·s·m^{-2}) stimulus. (A) Amplitudes of the *b* waveform of the scotopic rod responses. (B,C) *a* and *b* amplitudes of the cone-rod combined response revealed no significant differences after months of injection.

was chosen for further studies because E5C22E5 had more optical opacity than E4C20E4 by gross appearance.

The chemical structure of PEOz-PCL-PEOz was confirmed by ^{1}H NMR spectroscopy. All proton peaks of PEOz-PCL-PEOz were assigned, as indicated in Figure 1. The peak corresponding to the methyl protons in the repeated units of the PEOz segments was observed at 1.10 ppm, and the peak corresponding to the methylene carbon alpha to the ester group CH_2OCO in the repeated unit of the PCL segments was observed at 4.02 ppm.

Table 2. *a*-Wave and *b*-Wave Amplitudes and Implicit Times of Retinal ERG before and after ECE Hydrogel Injection[a]

scotopic ERG (rod)		*b*-wave [ms]	*b*-wave [μV]
ECE (before injection)		38.0 ± 0	135.3 ± 28.4
ECE (1 month after injection)		38.0 ± 2.2	156.8 ± 11.05
ECE (2 months after injection)		40.5 ± 5.2	142.9 ± 25.4
P value (1 month)		1.00	0.25
P value (2 months)		0.37	0.77
scotopic ERG (combined cone-rod)	*a*-wave [ms]	*b*-wave [ms]	*a*-wave [μV]	*b*-wave [μV]
ECE (before injection)	9.5 ± 1	33.5 ± 0.6	78.7 ± 9.0	158.5 ± 36.1
ECE (1 month after injection)	9.8 ± 1	34.3 ± 1.5	91.8 ± 10.3	183.8 ± 9.2
ECE (2 months after injection)	10.3 ± 1	34.3 ± 2.0	78.9 ± 3.4	165 ± 30.4
P value (1 month)	0.73	0.39	0.1	0.22
P value (2 months)	0.32	0.51	0.97	0.79

[a]Wilcoxon signed rank test.

The molecular weight and composition of the PEOz-PCL-PEOz triblock copolymer were determined from the ratio of the areas under the peaks at 1.10 and 4.02 ppm. The molecular weight and polydispersity of the PEOz, PEOz-PCL, and PEOz-PCL-PEOz were determined by GPC and are presented in Table 1. The GPC profiles of the PEOz, PEOz-PCL, and PEOz-PCL-PEOz block copolymers had a unimodal and narrow peak. The very narrow molecular weight distribution (polydispersity <1.3) demonstrated the effectiveness of the synthetic process. FTIR was also used to confirm the identities of the functional groups of the block copolymers. Together, the ^{1}H NMR, GPC, and FTIR results indicated that the triblock copolymer was successfully synthesized.

Sol−Gel Transition of ECE Hydrogel. The ECE hydrogel was prepared in BSS at 10−30% w/v. At 25 °C, the 10% w/v ECE hydrogel was a translucent solution. As the temperature increased, the PEOz segments became slightly dehydrated; then, the PEOz segments entangled, forming micelle aggregates. At the same time, the hydrophobicity of the PCL segments also increased with increasing temperature.[42] These results demonstrate the sol (room temperature)−gel (physiological temperature) phase transition behavior (Figure 2). The sol−gel phase diagram of ECE was constructed using various concentrations and temperatures. As the concentration of the PEOz-PCL-PEOz solution increased, the micelles aggregated more easily, and the arrangement of the molecules became more ordered (opaque state). When the temperature increased above that of the formation of the gel, the PEOz collapsed,[43] the hydrophobicity of ECE increased, and the block copolymer separated from the BSS.[44] From the sol−gel transition curve, the ECE hydrogel would be in solution form with the concentration below 10% w/v. The phenomenon of solution to gel transition in response to temperature change was observed in prepared 10, 15, and 20 wt % of ECE hydrogels solutions. Because the upper temperature limit of the gel phase in 10 and 15 wt % ECE hydrogel was 39 to 40 °C, close to the body temperature (37 °C), a 20 wt % ECE hydrogel was chosen for further study for a more stable gel at physiologic

dx.doi.org/10.1021/bm2009558 | *Biomacromolecules* 2012, 13, 40−48

body temperature to encapsulate bevacizumab for sustained drug release.

In Vitro Release of Bevacizumab from ECE Hydrogel. The extended in vitro release of bevacizumab from 20 wt % ECE hydrogel at 37 °C was investigated by enzyme immunoassay. Figure 3 shows the cumulative release profile. Bevacizumab was released at a constant rate of 40 μg/day for 11 days from the ECE hydrogel without a burst effect in its initial state. The release rate then declined. The primary mechanism for the release of a drug from biodegradable hydrogel has been proposed to have two phases. The first phase is chiefly determined by drug diffusion through the viscous hydrogel, and the second phase is the biodegradation of the hydrogel.[45,46] As the concentration gradient of bevacizumab between the external solution and gel declined, equilibrium was reached. When equilibrium was achieved, the only residual driving force of bevacizumab release was biodegradation of the hydrogel. In this study, we found that 80% of the bevacizumab was released from the ECE hydrogel in 20 days. It demonstrated the competency of the encapsulated bevacizumab release from the ECE hydrogel via diffusion-controlled in the initial phase (0–11 days) and combined erosion and diffusion-controlled in the second phase (12–20 days).

It is desirable to have a higher initial drug concentration (loading dose) for a better therapeutic effect.[2,3] On the contrary, it is not expected to have the initial burst release from the hydrogel–drug complex as a major source of the drug loss. Although, from the clinical point of view, a burst release at the beginning might not be an undesired event, it is also in a dilemma because of the premature exhaustion of the encapsulated bevacizumab in the hydrogel. Our result revealed that the ECE did not have the burst release for the loading initially at a high drug dosage. When combined with an extra loading injection of pure bevacizumab, the extended release from a packing gel system will still be beneficial and provide a potential for clinical applications.

Different diseases have different amounts of intraocular VEGF need to be "neutralized" by the anti-VEGF antibody with a very wide range. For example, neovascular retinal vein occlusion (median vitreous VEGF: 435 pg/mL) and proliferative diabetic retinopathy (1759 ± 1721 pg/mL) have a higher vitreous concentration of VEGF than neovascular macular degeneration.[47–49] Besides, different studies report different vitreous levels of VEGF. For example, in proliferative diabetic retinopathy, in 2009 Noma et al.[47] reported the vitreous level of VEGF was 1759 pg/mL, but in 1996 Wells et al.[49] reported 37.77 ng/mL. After a major neovascular inhibition by the "loaded" anti-VEGF, a smaller amount of anti-VEGF release in the vitreous would be enough for neutralizing the "daily released" VEGF. We believe that the sustained release of drugs would still be helpful for specific ocular neovascular diseases of less-than-super neovascular intensity.

Hydrolytic Degradation of ECE Hydrogel in BSS. Morphological observation by SEM of the hydrolytic degradation was conducted at 37 °C in BSS. Figure 4 shows the degradation profile of 20 wt % ECE hydrogel for 50 days. Initially, the surface morphology of the hydrogel was smooth, and the cross-section images showed exposed polymeric fibers. After 10 days of erosion, pores of 10–20 μm in size and channels were observed through which the drug could be released. After 50 days of erosion, the pores became larger and more numerous.

Evaluation of In Vitro Cytotoxicity by Flow Cytometry. The in vitro cytotoxicity of the ECE hydrogel was determined by coculturing the hydrogel with ARPE-19 cells for 24 h at 37 °C. Figure 5 shows the results. More than 90% of ARPE-19 cells, the well-known retinal cells from human source utilized for in vitro assays,[50] presented PI fluorescent negative. It indicates that 90% of the cocultured ARPE-19 cells were viable after the addition of different concentrations of ECE. In contrast, 70% of APRE-19 cells were PI fluorescent-positive in the presence of toxic particle (positive control group). The results were also confirmed by the trypan blue exclusion method with a hemocytometer and a microscope (data not shown).

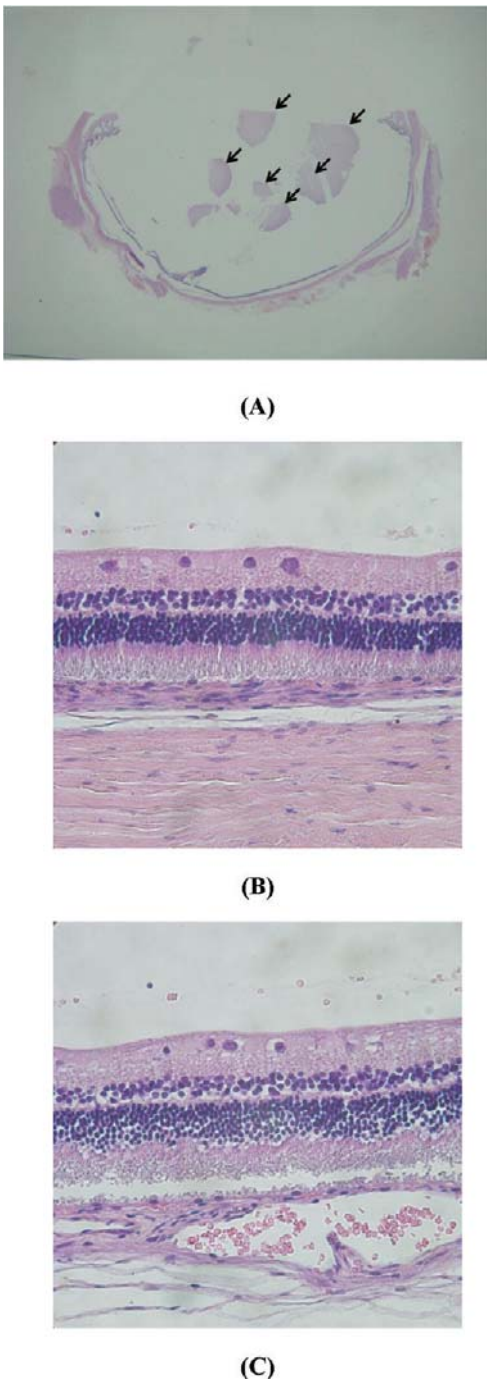

Figure 8. Histology of retinal sections of BSS-injected control eyes (B, 400×) and amphiphilic PEOz-PCL-PEOz-triblock-copolymer-injected eyes (A, 4×; C, 400×). The arrows indicate the residual ECE hydrogel in the vitreous cavity. The inner neuroretinal layer and outer photoreceptor layer are morphologically comparable between the study eyes and control eyes (hematoxylin and eosin stain).

dx.doi.org/10.1021/bm2009558 | *Biomacromolecules* 2012, 13, 40–48

Electroretinogram. The ECE hydrogel-BSS solution (500 μL, 1:1 v/v) was injected into the vitreous using a 27-gauge microinjector under a dissecting microscope. The in vivo cytotoxicity study in rabbit eyes by ERG for 2 months revealed *a* and *b* waveforms comparable to the waveforms before injection (Figure 6), demonstrating similar outer retinal (photoreceptor) and inner retinal (neurotransduction cells) function pre- and postinjection. Figure 7 shows the amplitudes of the *b* waveform of the scotopic rod responses and the *a* and *b* waves of the cone-rod combined response from three rabbits' eyes after intravitreal injection. Nonparametric statistics from a Wilcoxon signed rank test revealed no significant differences between the two groups ($n = 4$, $p > 0.05$) (Table 2). These results indicate that the functions of the whole layer of neuroretinal tissue were normal, even though the ECE hydrogel had been degrading in the vitreous fluid for 2 months, suggesting that the ECE hydrogel and its degradation products are not toxic to neuroretinal tissue, at least for 2 months.

Histology. Two months after injection, the rabbit eyes were enucleated for histological analysis. The hematoxylin and eosin staining results demonstrated a residual ECE hydrogel in the vitreous cavity, a normal retinal histology with no retinal necrosis, no infiltration of inflammatory cells and no morphological change between treated and untreated eyes. Precisely, the vulnerable inner neuroretinal layer and outer photoreceptor were morphologically comparable between study and control groups. These results demonstrate that the ECE hydrogel has low or no retinal toxicity (Figure 8).

CONCLUSIONS

A novel thermosensitive biodegradable ECE hydrogel was successfully synthesized and used as an intraocular carrier for bevacizumab. The ECE hydrogel exhibited a reversible sol−gel transition. It was found in a liquid form at room temperature, which facilitates mixing with the bevacizumab. However, it was found in a gel form at physiological temperature in which bevacizumab can be encapsulated for sustained release. Good in vitro and in vivo biocompatibility for the neuroretinal tissue was observed. The phase transition, biodegradability, good in vitro and intraocular biocompatibility, and extended drug release characteristics make the ECE hydrogel a candidate for biomedical and therapeutic applications.

AUTHOR INFORMATION

Corresponding Author

*E-mail: ghhsiue@mx.nthu.edu.tw; Tel: + 886-3-5719956; Fax: + 886-3-5726825 (G.-H.H.). E-mail: yihshiou.hwang@gmail.com; Tel: +886-3-3281200; Fax: +886-3-3287798 (Y.-S.H.).

Author Contributions

▽These authors contributed equally.

ACKNOWLEDGMENTS

This study was financially supported by grants from Chang Gung Memorial Hospital (CMRPG 380181, CMRPG 390311, CMRPD150382, and BMRP440) and the National Science Council (98-2622-E-033-011-CC1) and (99-2622-E-033-005-CC1) of the Republic of China, Taiwan. We gratefully acknowledge Ms. Y. Y. Kuo and Ms. S. T. Wu for their kind technical assistance and instrumental support from Chang Gung University and Chang Gung Memorial Hospital.

REFERENCES

(1) Carmeliet, P.; Ferreira, V.; Breier, G.; Pollefeyt, S.; Kieckens, L.; Gertsenstein, M.; Fahrig, M.; Vandenhoeck, A.; Harpal, K.; Eberhardt, C.; Declercq, C.; Pawling, J.; Moons, L.; Collen, D.; Risau, W.; Nagy, A. *Nature* **1996**, *380*, 435−439.

(2) Rosenfeld, P. J.; Brown, D. M.; Heier, J. S.; Boyer, D. S.; Kaiser, P. K.; Chung, C. Y.; Kim, R. Y. *N. Engl. J. Med.* **2006**, *355*, 1419−1431.

(3) Brown, D. M.; Kaiser, P. K.; Michels, M.; Soubrane, G.; Heier, J. S.; Kim, R. Y.; Sy, J. P.; Schneider, S. *N. Engl. J. Med.* **2006**, *355*, 1432−1444.

(4) Andreoli, C. M.; Miller, J. W. *Curr. Opin. Ophthalmol.* **2007**, *18*, 502−508.

(5) Willett, C. G.; Boucher, Y.; di Tomaso, E.; Duda, D. G.; Munn, L. L.; Tong, R. T.; Chung, D. C.; Sahani, D. V.; Kalva, S. P.; Kozin, S. V. *Nat. Med* **2004**, *10*, 145−147.

(6) Hurwitz, H.; Fehrenbacher, L.; Novotny, W.; Cartwright, T.; Hainsworth, J.; Heim, W.; Berlin, J.; Baron, A.; Griffing, S.; Holmgren, E. *N. Engl. J. Med.* **2004**, *350*, 2335−2342.

(7) Ferrara, N.; Hillan, K. J.; Gerber, H. P.; Novotny, W. *Nat. Rev. Drug. Discovery* **2004**, *3*, 391−400.

(8) Avery, R. L.; Pieramici, D. J.; Rabena, M. D.; Castellarin, A. A.; Nasir, M. A.; Giust, M. J. *Ophthalmology* **2006**, *113*, 363−372e365.

(9) Martin, D. F.; Maguire, M. G.; Ying, G. S.; Grunwald, J. E.; Fine, S. L.; Jaffe, G. J. *N. Engl. J. Med.* **2011**, *364*, 1897−1908.

(10) Raftery, J.; Clegg, A.; Jones, J.; Tan, S. C.; Lotery, A. *Br. J. Ophthalmol.* **2007**, *91*, 1244−1246.

(11) Krohne, T. U.; Eter, N.; Holz, F. G.; Meyer, C. H. *Am. J. Ophthalmol.* **2008**, *146*, 508−512.

(12) Regillo, C. D.; Brown, D. M.; Abraham, P.; Yue, H.; Ianchulev, T.; Schneider, S.; Shams, N. *Am. J. Ophthalmol.* **2008**, *145*, 239−248.

(13) Holz, F. G.; Amoaku, W.; Donate, J.; Guymer, R. H.; Kellner, U.; Schlingemann, R. O.; Weichselberger, A.; Staurenghi, G. *Ophthalmology* **2011**, *118*, 663−671.

(14) Fintak, D. R.; Shah, G. K.; Blinder, K. J.; Regillo, C. D.; Pollack, J.; Heier, J. S.; Hollands, H.; Sharma, S. *Retina* **2008**, *28*, 1395−1399.

(15) Kang Derwent, J. J.; Mieler, W. F. *Trans. Am. Ophthalmol. Soc.* **2008**, *106*, 206−214.

(16) Abrishami, M.; Ganavati, S. Z.; Soroush, D.; Rouhbakhsh, M.; Jaafari, M. R.; Malaekeh-Nikouei, B. *Retina* **2009**, *29*, 699−703.

(17) Carrasquillo, K. G.; Ricker, J. A.; Rigas, I. K.; Miller, J. W.; Gragoudas, E. S.; Adamis, A. P. *Invest. Ophthalmol. Visual Sci.* **2003**, *44*, 290−299.

(18) Ideta, R.; Tasaka, F.; Jang, W. D.; Nishiyama, N.; Zhang, G. D.; Harada, A.; Yanagi, Y.; Tamaki, Y.; Aida, T.; Kataoka, K. *Nano Lett.* **2005**, *5*, 2426−2431.

(19) Usui, T.; Sugisaki, K.; Amano, S.; Jang, W. D.; Nishiyama, N.; Kataoka, K. *Cornea* **2005**, *24*, S39−S42.

(20) Hsiue, G. H.; Chang, R. W.; Wang, C. H.; Lee, S. H. *Biomaterials* **2003**, *24*, 2423−2430.

(21) Turturro, S. B.; Guthrie, M. J.; Appel, A. A.; Drapala, P. W.; Brey, E. M.; Perez-Luna, V. H.; Mieler, W. F.; Kang-Mieler, J. J. *Biomaterials* **2011**, *32*, 3620−3626.

(22) Colthurst, M. J.; Williams, R. L.; Hiscott, P. S.; Grierson, I. *Biomaterials* **2000**, *21*, 649−665.

(23) Burdick, J. A.; Ward, M.; Liang, E.; Young, M. J.; Langer, R. *Biomaterials* **2006**, *27*, 452−459.

(24) Green, R. A.; Lovell, N. H.; Wallace, G. G.; Poole-Warren, L. A. *Biomaterials* **2008**, *29*, 3393−3399.

(25) Misra, G. P.; Singh, R. S. J.; Aleman, T. S.; Jacobson, S. G.; Gardner, T. W.; Lowe, T. L. *Biomaterials* **2009**, *30*, 6541−6547.

(26) Anumolu, S. N. S.; DeSantis, A. S.; Menjoge, A. R.; Hahn, R. A.; Beloni, J. A.; Gordon, M. K.; Sinko, P. J. *Biomaterials* **2010**, *31*, 964−974.

(27) Ballios, B. G.; Cooke, M. J.; van der Kooy, D.; Shoichet, M. S. *Biomaterials* **2010**, *31*, 2555−2564.

(28) Park, K. H.; Na, K.; Kim, S. W.; Jung, S. Y.; Chung, H. M. *Biotechnol. Lett.* **2005**, *27*, 1081−1086.

(29) Li, J.; Li, X.; Ni, X.; Wang, X.; Li, H.; Leong, K. W. *Biomaterials* **2006**, *27*, 4132−4140.

(30) Loh, X. J.; Goh, S. H.; Li, J. *Biomaterials* **2007**, *28*, 4113−4123.
(31) Jeong, B.; Bae, Y. H.; Lee, D. S.; Kim, S. W. *Nature* **1997**, *388*, 860−862.
(32) Jeong, B.; Choi, Y. K.; Bae, Y. H.; Zentner, G.; Kim, S. W. *J. Controlled Release* **1999**, *62*, 109−114.
(33) Luxenhofer, R.; Schulz, A.; Roques, C.; Li, S.; Bronich, T. K.; Batrakova, E. V.; Jordan, R.; Kabanov, A. V. *Biomaterials* **2010**, *31*, 4972−4979.
(34) Gaertner, F. C.; Luxenhofer, R.; Blechert, B.; Jordan, R.; Essler, M. *J. Controlled Release* **2007**, *119*, 291−300.
(35) Mero, A.; Pasut, G.; Via, L. D.; Fijten, M. W. M.; Schubert, U. S.; Hoogenboom, R.; Veronese, F. M. *J. Controlled Release* **2008**, *125*, 87−95.
(36) Athanasiou, K. A.; Niederauer, G. G.; Agrawal, C. *Biomaterials* **1996**, *17*, 93−102.
(37) Lee, S. C.; Kang, S. W.; Kim, C.; Kwon, I. C.; Jeong, S. Y. *Polymer* **2000**, *41*, 7091−7097.
(38) Lee, S. C.; Chang, Y.; Kim, C.; Kwon, I. C.; Kim, Y. H.; Jeong, S. Y. *Macromolecules* **1999**, *32*, 1847−1852.
(39) Shen, C. R.; Wu, S. T.; Tsai, Z. T.; Wang, J. J.; Yen, T. C.; Tsai, J. S.; Shih, M. F.; Liu, C. L. *Polym. Int.* **2011**, *60*, 945−950.
(40) Gjorloff, K.; Andreasson, S.; Ehinger, B. *Doc. Ophthalmol.* **2004**, *109*, 163−168.
(41) Weber, C.; Becer, R. C.; Baumgaertel, A.; Hoogenboom, R.; Schubert, U. S. *Des. Monomers Polym.* **2009**, *12*, 149−165.
(42) Huynh, C. T.; Nguyen, M. K.; Lee, D. S. *Macromolecules* **2011**, *44*, 6629−6636.
(43) Loh, X. J.; Goh, S. H.; Li, J. *Biomacromolecules* **2007**, *8*, 585−593.
(44) Hyun, H.; Kim, Y. H.; Song, I. B.; Lee, J. W.; Kim, M. S.; Khang, G.; Park, K.; Lee, H. B. *Biomacromolecules* **2007**, *8*, 1093−1100.
(45) Sharifpoor, S.; Amsden, B. *Eur. J. Pharm. Biopharm.* **2007**, *65*, 336−345.
(46) Amsden, B. G.; Timbart, L.; Marecak, D.; Chapanian, R.; Tse, M. Y.; Pang, S. C. *J. Controlled Release* **2010**, *145*, 109−115.
(47) Noma, H.; Funatsu, H.; Mimura, T.; Harino, S.; Hori, S. *Ophthalmology* **2009**, *116*, 87−93.
(48) Ambati, J.; Chalam, K. V.; Chawla, D. K.; D'Angio, C. T.; Guillet, E. G.; Rose, S. J.; Vanderlinde, R. E.; Ambati, B. K. *Arch. Ophthalmol.* **1997**, *115*, 1161−1166.
(49) Wells, J. A.; Murthy, R.; Chibber, R.; Nunn, A.; Molinatti, P. A.; Kohner, E. M.; Gregor, Z. J. *Br. J. Ophthalmol.* **1996**, *80*, 363−366.
(50) Narayanan, R.; Mungcal, J. K.; Kenney, M. C.; Seigel, G. M.; Kuppermann, B. D. *Invest. Ophthalmol. Visual Sci.* **2006**, *47*, 722−728.